

Supplement of Biogeosciences, 16, 1525–1542, 2019  
<https://doi.org/10.5194/bg-16-1525-2019-supplement>  
© Author(s) 2019. This work is distributed under  
the Creative Commons Attribution 4.0 License.



*Supplement of*

## **Atmospheric deposition fluxes over the Atlantic Ocean: a GEOTRACES case study**

**Jan-Lukas Menzel Barraqueta et al.**

*Correspondence to:* Jan-Lukas Menzel Barraqueta ([jmenzel@sun.ac.za](mailto:jmenzel@sun.ac.za))

The copyright of individual parts of the supplement might differ from the CC BY 4.0 License.

**Table S1.****Biogeochemical provinces and their principal characteristics used in this study from Longhurst (2010)**

Region	Acronym	Cruise	North boundary	South Boundary	East Boundary	West Boundary	Ecology	Physical properties
North Atlantic Subtropical	NAST	GA01	42° N SE flowing Azores Current	25-30° N Subtropical convergence	Canary current	Gulf Stream	Seasonal mixing, low productivity spring bloom (April-June)	Northern part of the anticyclonic gyre, light westerly winds and eddy fields in north, Moderate winter mixing (MLD 100-150 m)
North Atlantic Drift	NADR	GA01	56° N Oceanic Polar Front and Subarctic Front	42° N Meeting of NAD with southeast flowing Azores Current	European shelf break	45° W	Spring stratification and high production bloom (mid-April, 39-50 °N)	West wind drift, deep winter mixing (MLD < 200 m)
Atlantic Arctic	ARCT	GA01	Spitzbergen	Flemish Cap	North America	45° W	Large spring phytoplankton blooms.	Comprises the two cyclonic Subpolar Gyres of the North Atlantic Ocean. Deep winter mixing.
North Atlantic Tropical Gyral	NATR	GA06	~30 °N Subtropical convergence	10-12 °N Conjunction of Northern Equatorial Current and Countercurrent	Canary current	Bahama Islands	No spring bloom, low productivity and chlorophyll	Weak winter mixing, shallow MLD (15-120 m)
Western Tropical Atlantic	WTRA	GA06	~10 °N Northern Equatorial Countercurrent	~ 4 °S South Equatorial Current	20 °W	Brazilian shelf	No spring bloom and high spatial variability in production. High chlorophyll with high nutrient concentrations	Easterly trade winds and intertropical convergence zone (ITCZ), upwelling and seasonally variable Northern Equatorial Countercurrent
Eastern Tropical Atlantic	ETRA	GA08	5-10° N	5-10°S	15° W Shelfbreak front along the north-south coast from Cameroon to Congo	Shelf-edge front of the east-west coast of West Africa (Guinea to Nigeria)	Enhanced chlorophyll	Southeasterly trade-winds, ITCZ above the northwest corner in winter. Seasonally varying MLD as a consequence of changes in zonal wind stress.

South Atlantic Gyral	SATL	GA08	~ 4 °S South Equatorial Current	~40 °S Subtropical Convergence Province (raised chlorophyll by ~0.3 mg m <sup>-3</sup> )	Benguela current	Brazil current	Low surface chlorophyll. Highly productive eddies near boundaries	Shallow winter mixing, anticyclonic gyre, trade winds dominate, high pressure cell (20-30 °S). Greatest MLDs (<100 m) at ~ 20 °S. Westerly Brazil current south of gyre (35-42 °S)
Guinea Current Coastal	GUIN	GA08	12° N Cape Roxo	18° S Cape Frio	West African tropical coast along Congo and Angola	Shelf edge front at ca. 2-3° N 4° W	Oligotrophic area.	Shallow mixed layer above sharp and permanent thermocline. Strongly seasonal reversal of wind patterns.
Benguela Coastal Current	BENG	GA08	18° S	Cape of Good Hope	Southwestern Africa shelf	SATL region	High primary productivity.	Agulhas retroflexion area. Large upwelling area
Eastern Africa Coastal	EAFR	GA10	5° S Coastal boundary of Indian Ocean	Cape of Good Hope	Western boundary currents	BENG	High seasonal variability in chlorophyll concentrations	Shelf region with seasonal variability. Retroflexion of the Agulhas Current
South Subtropical Convergence	SSTC	GA10	35° S South Atlantic Gyre	45° S ACC	FKLD	EAFR	High nutrient low chlorophyll. Enhanced phytoplankton biomass in austral spring and midsummer.	Between anticyclonic circulation of the South Atlantic and cyclonic circulation of the Antarctic circumpolar Current. Strong convergence and downwelling occurring
South West Atlantic Shelf	FKLD	GA10	38° S Mar del Plata	55° S Tierra del Fuego	Argentine shelf and Falklands plateau	SSTC	High seasonal variability in chlorophyll concentrations	Subantarctic Front and confluence of Brazil Current and Malvinas Current



1 **Table S2:**

2 **Sampling and analysis approaches used for each of the cruises**

Cruise	Sampling CTD	Bottle	Filter type	Pore size	Air vs N <sub>2</sub>	Reference material	Values measured reference material (nM)
GA01	Trace metal clean Rosette (TMR, General Oceanics Inc. Model 1018 Intelligent Rosette)	GO-FLO	Sartobran 300, Sartorius	0.2 μM	N <sub>2</sub> (0.5 bar)	GD Safe S	17.79 ± 0.26 (n=4) 1.85 ± 0.33 (n=9)
GA06	Titanium frame clean CTD Rosette	10 L Teflon coated OTE	AcroPak Supor filter capsule (Pall Corp.)	0.2 μM	Oxygen free N <sub>2</sub> (0.1-0.5 bar)	GD GS	18.8 ± 0.8 (n=4) 28 ± 5 (n=7)
GA08	Trace metal clean CTD Rosette	12 L GO-FLO (OTE)	Acropak 500 cartridge filters (Pall Corp.)	0.2-0.8 μM	N <sub>2</sub> (0.2 bar)	GS	27.8 ± 0.2 (n=4)
GA10	Titanium frame clean CTD Rosette	10 L Teflon coated OTE	AcroPak Supor polyethersulfone membrane filter capsules (Pall Corp.)	0.2 μM	High purity air (1.7 bar)	SAFe S SAFe D2	1.68 ± 0.49 (n=3) 0.89 ± 0.09 (n=4)

3

4

5 **Table S3:**

6 **Definition of the regions based on Baker et al., (2013) to derive Al fractional solubility. Figure S1 shows the**  
 7 **location of the aerosol source region and air mass type sub-regions. The last column displays the weighted**  
 8 **average for Al fractional solubility. The different air mass types are as follow: NAr, North Atlantic remote; NAM,**  
 9 **North America; SAf, South African; SAR, South Atlantic remote; SAbb, South African burning biomass; Sah,**  
 10 **Saharan; SAm, South American.**

Cruise	Stations	Aerosol source region	Air mass type sub-region	Air mass type %	Al fractional solubility percentage
GA01	1 to 26	2	2a	NAr 77 European 15 NAm 8	11.6
GA01	29 to 71	-	-	NAr	21
GA01	77 and 78	-	-	Canadian	14.5
GA06	7 to 9	3	3b	SAf 47 SAR 44 SAbb 7	5.8

GA06	10	4	4a	Saf 82 SAbb 17	5.5
GA06	11.5 to 18	3	3a	NAr 31 Sah 21 SAf 25 SAbb 16	5
GA06	19 and 20	2	2d	Sah 48 NAr 46 Eur 6	8.6
GA08	1 to 5 & 30 to 52	4	4c	SAr 81 SAf 14 SAbb 5	10.3
GA08	6 to 29	4	4b	SAf 44 SAbb 31 SAr 25	7.7
GA10	1 to 3	4	4d	SAr 94	10.9
GA10	7 to 24	5	5b	SAr 52 SAm 45	13.9

11

12

13 **Table S4:**

14 **Columns 3 to 7: Calculated mixed layer depth (MLD, m), average measured dAl concentrations within the MLD**  
 15 **(nM), derived atmospheric deposition fluxes ( $\text{g m}^{-2}\text{yr}^{-1}$ ) for each of the stations along the four cruises, residence**  
 16 **time of dAl within the MLD (yr), and fractional aerosol Al solubility range (%).**

Cruise	Station number	MLD	dAl	Deposition flux	Residence time	Solubility range %
GA01	1	35.8	15.8	1.2	1.25	11.6-20
GA01	2	31.4	19.6	1.5	1.25	11.6-20
GA01	4	33.4	19.4	1.4	1.25	11.6-20
GA01	11	52.1	5.3	0.4	1.25	11.6-20
GA01	13	45.9	4.0	0.3	1.25	11.6-20
GA01	15	51.9	2.9	0.2	1.25	11.6-20
GA01	17	52.1	1.5	0.1	1.25	11.6-20
GA01	19	52.4	2.6	0.2	1.25	11.6-20
GA01	21	67.5	4.9	0.4	1.25	11.6-20
GA01	23	72.1	4.1	0.3	1.25	11.6-20
GA01	25	82.0	5.2	0.4	1.25	11.6-20
GA01	26	78.2	1.8	0.1	1.25	11.6-20
GA01	29	64.3	1.3	0.1	1.25	11.6-20
GA01	32	62.0	3.2	0.2	1.25	11.6-20
GA01	34	78.5	3.7	0.3	1.25	11.6-20
GA01	36	97.5	3.1	0.2	1.25	11.6-20
GA01	38	97.4	3.9	0.3	1.25	11.6-20
GA01	40	82.5	3.1	0.2	1.25	11.6-20

GA01	42	78.7	1.1	0.1	1.25	11.6-20
GA01	44	89.9	0.9	0.1	1.25	11.6-20
GA01	49	124.5	3.2	0.2	1.25	11.6-20
GA01	53	51.6	10.4	0.8	1.25	11.6-20
GA01	56	91.3	1.8	0.1	1.25	11.6-20
GA01	60	84.6	3.7	0.3	1.25	11.6-20
GA01	61	78.9	6.7	0.5	0.75	11.6-20
GA01	63	116.4	3.6	0.3	0.75	11.6-20
GA01	64	76.1	1.5	0.1	0.75	11.6-20
GA01	68	124.1	2.8	0.2	0.75	11.6-20
GA01	69	106.5	1.8	0.1	0.75	11.6-20
GA01	71	60.6	2.3	0.2	0.75	11.6-20
GA01	77	20.7	1.6	0.1	0.75	11.6-20
GA01	78	12.0	0.9	0.1	0.75	11.6-20
GA06	7	35.6	15.6	2.2	1.25	5-8.6
GA06	8	46.4	8.1	1.1	1.25	5-8.6
GA06	9	42.4	24.0	3.4	1.25	5-8.6
GA06	10	51.3	8.8	1.2	1.25	5-8.6
GA06	11.5	43.4	15.0	2.1	1.25	5-8.6
GA06	12	32.6	17.3	2.5	1.25	5-8.6
GA06	13	29.4	21.0	3.0	1.25	5-8.6
GA06	14	32.9	67.5	9.6	1.25	5-8.6
GA06	15	39.9	35.6	5.1	1.25	5-8.6
GA06	16	42.1	22.4	3.2	1.25	5-8.6
GA06	17	44.1	19.7	2.8	1.25	5-8.6
GA06	18	40.5	31.5	4.5	1.25	5-8.6
GA06	19	50.4	24.8	3.5	1.25	5-8.6
GA06	20	38.0	16.6	2.4	1.25	5-8.6
GA08	1	-	-	-	-	
GA08	2	-	-	-	-	
GA08	3	33.0	4.4	0.8	0.75	7.7-10.3
GA08	4	59.0	4.0	0.7	0.75	7.7-10.3
GA08	5	29.0	4.9	0.9	0.75	7.7-10.3
GA08	6	13.0	12.0	2.2	0.75	7.7-10.3
GA08	7	25.2	22.0	4.1	0.75	7.7-10.3
GA08	8	12.2	31.0	5.7	0.75	7.7-10.3
GA08	9	13.5	43.0	7.9	0.75	7.7-10.3
GA08	10	14.1	62.0	11.4	0.75	7.7-10.3
GA08	11	11.8	14.5	2.7	0.75	7.7-10.3
GA08	12	11.0	28.0	5.2	0.75	7.7-10.3
GA08	13	8.5	72.0	13.3	0.75	7.7-10.3
GA08	14	12.0	37.0	6.8	0.75	7.7-10.3
GA08	15	13.0	784.6	163.2	0.75	7.7-10.3

GA08	16	5.0	269.0	56.0	0.75	7.7-10.3
GA08	17	8.7	261.0	54.3	0.75	7.7-10.3
GA08	18	9.2	211.0	43.9	0.75	7.7-10.3
GA08	19	8.2	209.0	43.5	0.75	7.7-10.3
GA08	20	9.0	186.0	38.7	0.75	7.7-10.3
GA08	21	15.8	44.9	8.3	0.75	7.7-10.3
GA08	22	20.2	48.6	9.0	0.75	7.7-10.3
GA08	23	23.8	32	6.7	0.75	7.7-10.3
GA08	24	28.4	20.8	3.8	0.75	7.7-10.3
GA08	25	37.2	13.6	2.5	0.75	7.7-10.3
GA08	26	24.8	7.0	1.3	0.75	7.7-10.3
GA08	27	28.0	9.8	1.8	3	7.7-10.3
GA08	28	40.4	12.8	2.4	3	7.7-10.3
GA08	29	30.0	7.3	1.3	3	7.7-10.3
GA08	30	56.4	11.8	2.2	3	7.7-10.3
GA08	31	41.7	4.5	0.8	3	7.7-10.3
GA08	32	44.6	1.8	0.3	3	7.7-10.3
GA08	33	35.4	2.3	0.4	3	7.7-10.3
GA08	34	39.2	5.3	1.0	3	7.7-10.3
GA08	35	40.5	4.3	0.8	3	7.7-10.3
GA08	36	32.3	1.9	0.3	3	7.7-10.3
GA08	37	35.5	2.2	0.4	3	7.7-10.3
GA08	38	38.6	1.5	0.3	3	7.7-10.3
GA08	39	43.6	1.9	0.4	0.75	7.7-10.3
GA08	40	-	-	-		
GA08	41	42.0	2.5	0.5	0.75	7.7-10.3
GA08	42	31.8	5.4	1.0	0.75	7.7-10.3
GA08	43	34.0	3.3	0.6	0.75	7.7-10.3
GA08	44	6.0	1.2	0.2	0.75	7.7-10.3
GA08	45	36.1	4.3	0.8	0.75	7.7-10.3
GA08	46	65.0	2.9	0.5	0.75	7.7-10.3
GA08	47	12.0	8.3	1.5	0.75	7.7-10.3
GA08	48	11.0	2.2	0.4	0.75	7.7-10.3
GA08	49	12.0	4.9	0.9	0.75	7.7-10.3
GA08	50	12.0	4.7	0.8	0.75	7.7-10.3
GA08	51	19.0	4.5	0.7	0.75	7.7-10.3
GA10	1	29.3	4.4	0.3	1.5	10.9-13.9
GA10	2	32.4	4.2	0.4	1.5	10.9-13.9
GA10	3	54.4	0.7	0.0	1.5	10.9-13.9
GA10	7	65.4	0.4	0.0	1	10.9-13.9
GA10	8	54.1	0.7	0.1	1	10.9-13.9
GA10	11	62.8	0.3	0.0	1	10.9-13.9
GA10	12	65.1	1.9	0.1	1	10.9-13.9

GA10	13	65.4	0.5	0.0	1	10.9-13.9
GA10	14	48.1	0.7	0.1	1	10.9-13.9
GA10	15	56.2	0.7	0.1	1	10.9-13.9
GA10	16	69.9	1.6	0.1	1	10.9-13.9
GA10	17	71.8	2.7	0.2	1	10.9-13.9
GA10	18	57.9	2.0	0.1	1	10.9-13.9
GA10	19	51.6	1.1	0.1	1	10.9-13.9
GA10	20	30.5	5.2	0.3	1	10.9-13.9
GA10	21	46.0	12.0	0.8	1	10.9-13.9
GA10	22	34.0	15.8	1.0	1	10.9-13.9
GA10	24	28.1	5.4	0.3	1	10.9-13.9

17

18

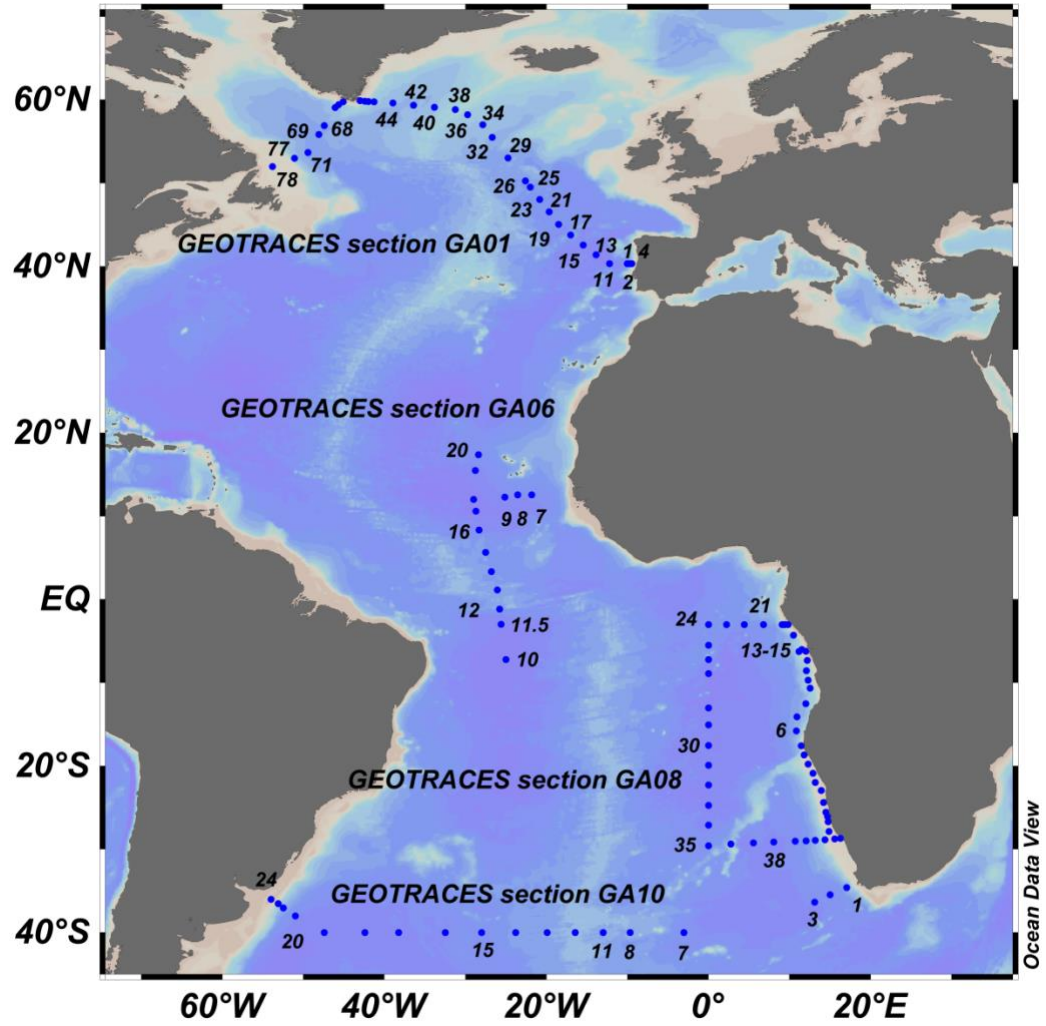
19

20

21

22

23



24

25

26 **Figure S1**

27 **Map showing the cruise locations and station numbers**

28

29

30

31

32

33

34

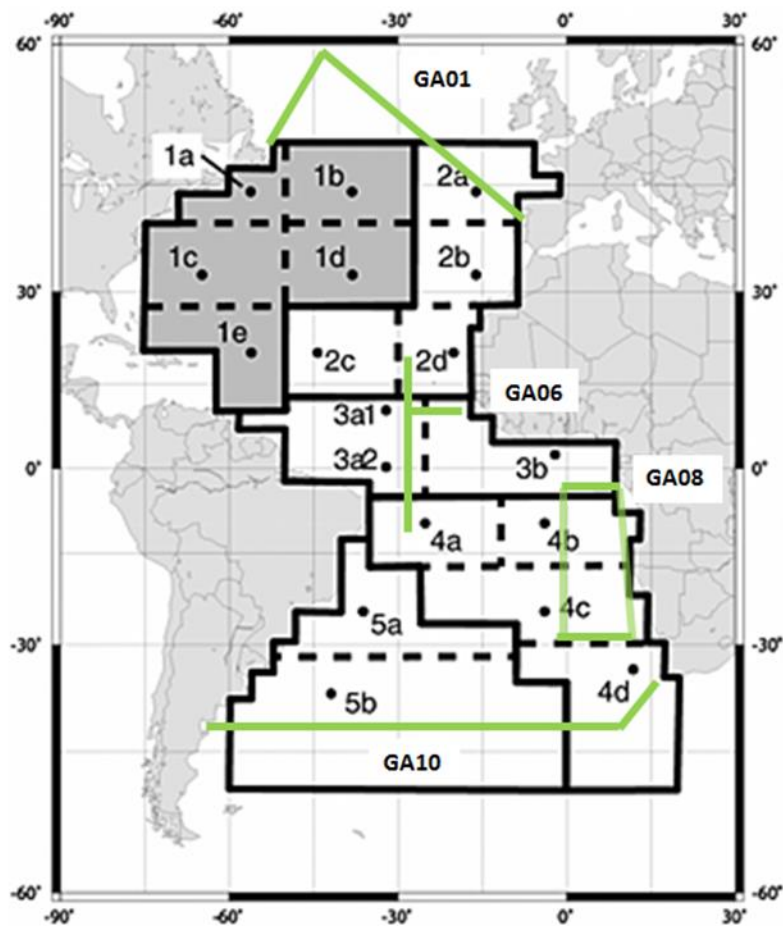


**Figure S2:**

**Atmospheric sub-regions used to define aerosol AI fractional solubility. The cruise tracks for GA01, GA06, GA08 and GA10 are plotted as green solid lines. Modified from (Baker et al., 2013).**

**Explanatory notes for Figure S2:**

**Fractional AI solubility in the North Atlantic (GA01)**

In the North Atlantic, section GA01, we used a combination of in AI fractional solubility ( $AI_{sol\%}$ ) estimates from aerosols collected during the cruise (Shelley et al., 2017) for stations north of 50°N and  $AI_{sol\%}$  estimates from the compilation of Baker et al. (2013) for stations south of 50°N. For stations 1 to 26 we used an  $AI_{sol\%}$  of 11.6 % as the stations fall into aerosol source region 2 and air mass type sub-region 2a. Sub region 2a is dominated by North Atlantic remote (76.8 %) and European (15.2 %) air mass types with a small and residual contribution of North American (7.8 %) and Saharan (0.25 %) air mass types, respectively. From station 29 to 71 we averaged all the aerosol  $AI_{sol\%}$  estimates as all the air mass types for the aerosol samples collected ( $n=9$ ) between the previous mentioned stations had a North Atlantic remote air mass provenance yielding a final  $AI_{sol\%}$  of 21 %. The last two stations (77 and 78) were located between aerosol samples geoa17 and geoa18 which had a Canadian air mass type origin with an average  $AI_{sol\%}$  of 14.5 %.

**Fractional AI solubility in the tropical Atlantic (GA06)**

For the tropical Atlantic, section GA06, we selected four different  $AI_{sol\%}$  values. For the eastward transect (stations 7 to 9) an  $AI_{sol\%}$  of 5.8 % was selected as the stations were located in the aerosol source region number 3. Air mass

66 provenance within sub-region 3b were Southern African (46.5%) and South Atlantic remote (43.6%), with a small  
67 contribution of Southern African biomass burning (7.1%) and Sahara (2.7%) air mass types and a residual  
68 contribution of North Atlantic remote (0.2%) air mass type. The most southern station (station 10) was located  
69 within source region 4 and air mass provenance within sub-region 4a. Sub-region 4a was dominated by Southern  
70 African (82.1%) and Southern African biomass burning (16.9%) air mass types with an additional small contribution  
71 of Southern Atlantic remote (1.1%) air mass type, thus yielding an  $Al_{sol\%}$  of 5.5 %. Similar to station 10, for the  
72 northward transect (St. 11.5 to 18) we used an  $Al_{sol\%}$  of 5 %. This northward transect was located in aerosol source  
73 region 3, although the air mass type provenance was a combination between sub regions 3a1 and 3a2. Sub-region  
74 3a (3a1+3a2) had a mixed air mass type provenance, with North Atlantic remote (30.5 %), Sahara (20.7 %),  
75 Southern African (24.9 %) and Southern Atlantic biomass burning (15.5 %) dominating the air mass types. A small  
76 contribution of Southern Atlantic remote (9.1 %) and European (0.2 %) was also present. The most northern  
77 stations (St. 19 and 20) had the highest  $Al_{sol\%}$  with a value of 8.6 % as they were located in aerosol source region 2  
78 and air mass type provenance sub-region 2d, which is dominated by Sahara (48.1. %) and North Atlantic remote  
79 (45.7 %) air mass types. Sub-region 2d also had a small and residual contribution of European (6 %) and North  
80 American (0.3 %) air mass types, respectively.

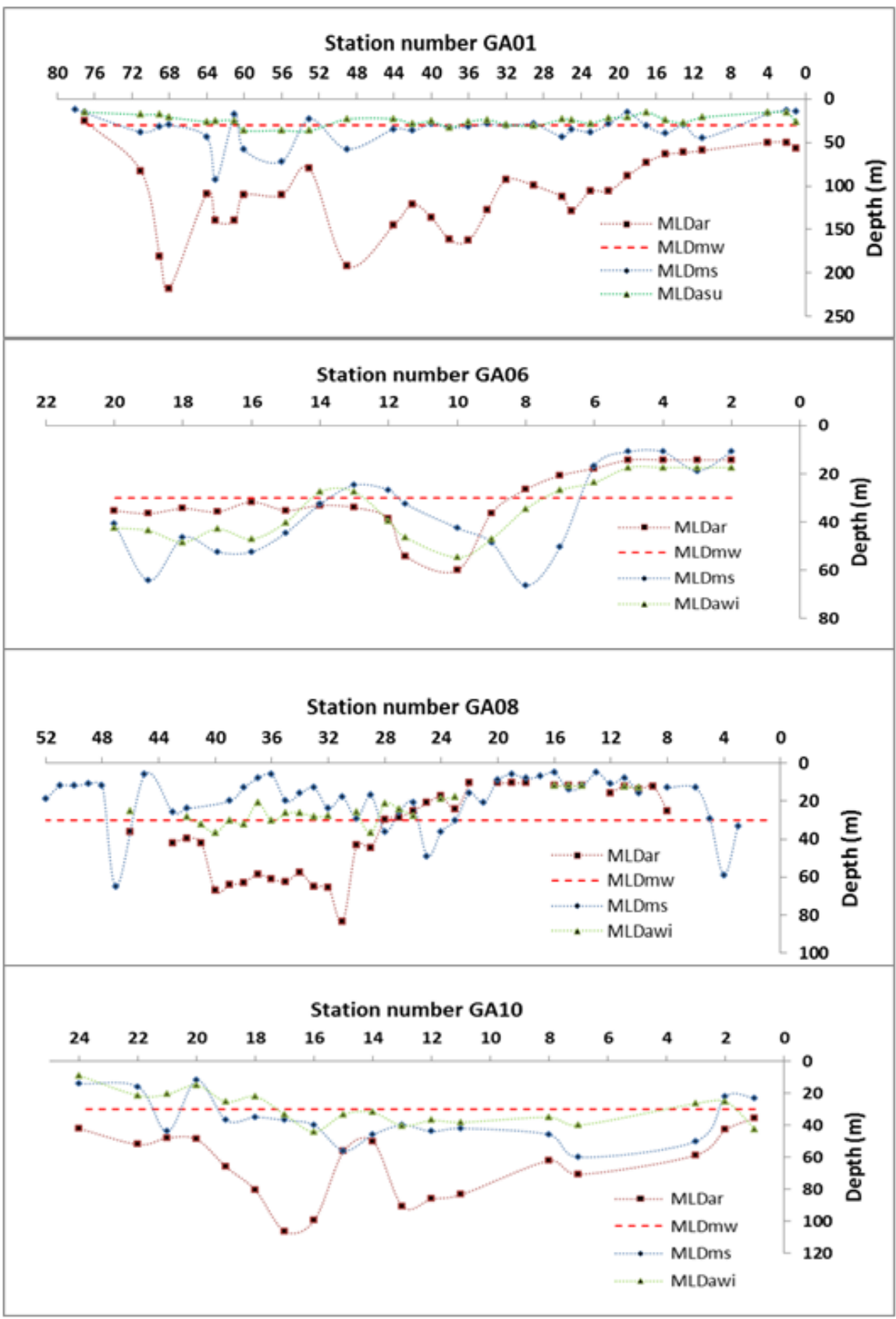
#### 81 **Fractional $Al_{sol\%}$ in the South East Atlantic (GA08)**

82 In the South East Atlantic, section GA08, two different  $Al_{sol\%}$  were used. Both were located in aerosol source region  
83 4. Stations 1 to 5 and 30 to 52 were located in air mass type sub-region 4c. Sub-region 4c was dominated by  
84 Southern Atlantic remote (81.2 %) and South African (13.5 %) air mass types with smaller contributions of  
85 Southern Africa burning biomass (4.9 %) and South American (0.5 %) air mass types, yielding an average  $Al_{sol\%}$  of  
86 10.3 %. Stations 6 to 29 were located in air mass type sub-region 4b, where the dominant air type masses were  
87 Southern Africa (44.2 %), Southern Africa burning biomass (30.8 %) and Southern Atlantic remote (25.1 %).  
88 Average  $Al_{sol\%}$  for sub-region 4b was 7.7 %.

#### 89 **Fractional $Al_{sol\%}$ in the South Atlantic Ocean (GA10)**

90 For the Southern Ocean (GA10), two different  $Al_{sol\%}$  were used. On the eastern part of the transect, stations 1 to 3,  
91 we used a value of 10.9 % which is mainly due to 94.3 % of the air masses types having a South Atlantic remote  
92 areas origin with an average  $Al_{sol\%}$  of 11.3. West of station 3, stations 7 to 24, we used an  $Al_{sol\%}$  of 13.9 % which is  
93 mainly due to the combined effect of 52 % and 45 % of the air masses coming from South Atlantic marine remote  
94 areas and South America with an average  $Al_{sol\%}$  of 14.1 % and 14.5 %, respectively.

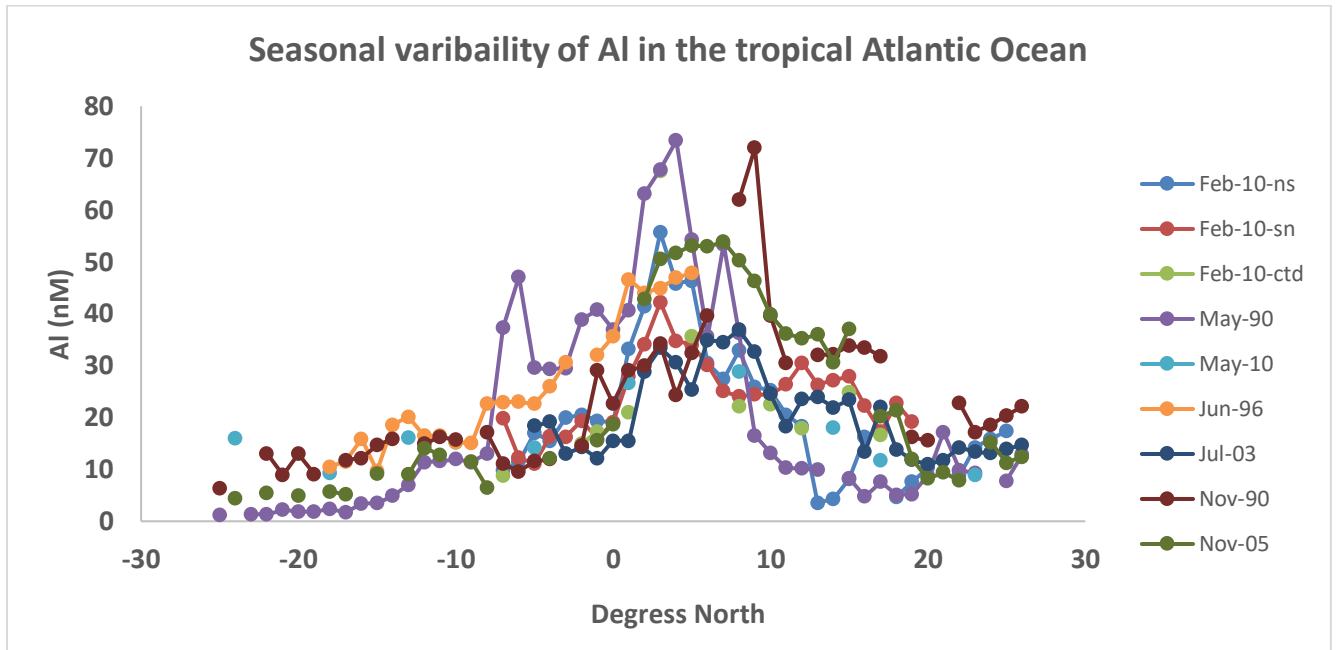
95



96 Figure S3

97 Depth of the surface mixed layer (MLD). MLDar refers to the annual average MLD from the Argo project (Holte  
 98 et al., 2017). MLDms refers to in situ MLD measured on each cruise. MLDasu or MLDawi represent the summer

99 or winter average MLD from the Argo project. MLDmw represent the MLD used in the original application of the  
100 MADCOW model (30 m) (Measures et al., 2015).



101

102 **Figure S4**

103 The legend represents month and year when the different cruises took place. Feb-10-ns, Feb-10-sn, and Feb-10-  
104 ctd are samples taken during the same expedition. Ns and sn refer to north-south and south-north transects  
105 respectively (samples taken with a tow-fish) while ctd refers to samples taken from Go-Flo bottles. References  
106 associated to each cruise are as follow: (i) Feb-10-ns and Feb-10-sn (Schlosser et al., 2014); (ii) Feb-10-ctd (this  
107 study); (iii) May-90 and Nov-90 (Helmert and Van der Loeff, 1993); (iv) May-10 (Dammshäuser et al., 2011); (v)  
108 Jun-96 (Vink and Measures, 2001); (vi) Jul-03 (Measures et al., 2008).

109

110

111

112

113

114

115

116

117

118

119

120

121

122

123

124

125

126

127

128

129

130

131

132

133

134

135

136

137 **Figure S5**

138 **Chlorophyll-a concentrations throughout GEOTRACES section GA08. Unpublished data from Thomas J. Browning.**

139 **Coulored circles represent chlorophyll-a concentrations. The background colouring represents world ocean**

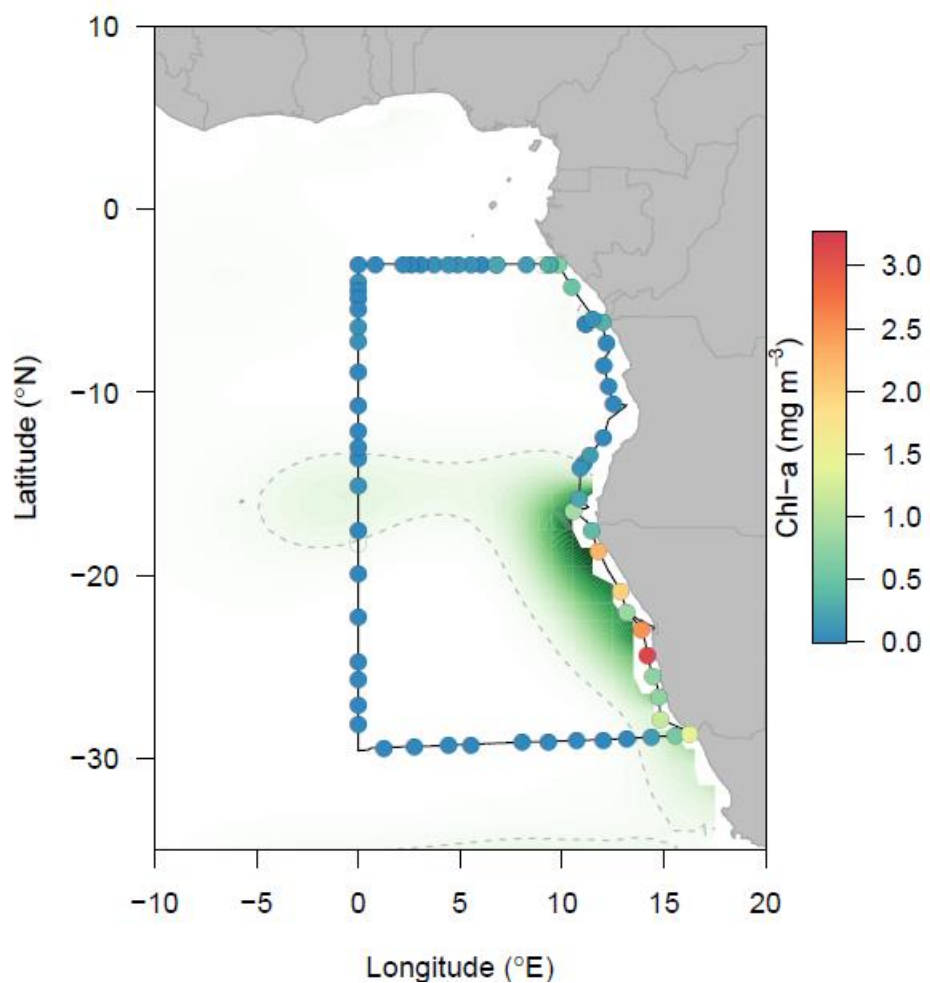
140 **atlas nitrate for December on a relative scale (darker green indicates higher nitrate, dashed line indicates 1uM**

141 **nitrate contour).**

142

143

144



145

146 **References**

147

148 Baker, A., Adams, C., Bell, T., Jickells, T., and Ganzeveld, L. (2013). Estimation of atmospheric nutrient inputs to  
149 the Atlantic Ocean from 50° N to 50° S based on large-scale field sampling: Iron and other dust-  
150 associated elements. *Global Biogeochemical Cycles*, 27(3), 755-767, 2013

151 Dammshäuser, A., Wagener, T., and Croot, P. L. (2011). Surface water dissolved aluminum and titanium: Tracers  
152 for specific time scales of dust deposition to the Atlantic? *Geophysical Research Letters*, 38(24), 2011

153 Helmers, E., and Rutgers van der Loeff, M. M. (1993). Lead and aluminum in Atlantic surface waters (50 N to 50  
154 S) reflecting anthropogenic and natural sources in the eolian transport. *98(C11)*, 20261-20273, 1993

155 Holte, J., Talley, L. D., Gilson, J., and Roemmich, D. (2017). An Argo mixed layer climatology and database.  
156 *Geophysical Research Letters*, 44(11), 5618-5626, 2017

157 Longhurst, A. R.: Ecological geography of the sea, Academic Press, Elsevier, 560 pp., 2010.

158 Measures, C., Hatta, M., Fitzsimmons, J., and Morton, P. (2015). Dissolved Al in the zonal N Atlantic section of  
159 the US GEOTRACES 2010/2011 cruises and the importance of hydrothermal inputs. *Deep Sea Research*  
160 *Part II: Topical Studies in Oceanography*, 116, 176-186, 2015

161 Schlosser, C., Klar, J. K., Wake, B. D., Snow, J. T., Honey, D. J., Woodward, E. M. S., Lohan, M. C., Achterberg, E.  
162 P., and Moore, C. M. (2014). Seasonal ITCZ migration dynamically controls the location of the  
163 (sub)tropical Atlantic biogeochemical divide. *Proceedings of the National Academy of Sciences*, 111(4),  
164 1438-1442, 2014

165 Shelley, R. U., Landing, W. M., Ussher, S. J., Planquette, H., and Sarthou, G.: Regional trends in the fractional  
166 solubility of Fe and other metals from North Atlantic aerosols (GEOTRACES cruises GA01 and GA03)  
167 following a two-stage leach, *Biogeosciences*, 15, 2271-2288, 2018.

168 Vink, S., and Measures, C. I. (2001). The role of dust deposition in determining surface water distributions of Al  
169 and Fe in the South West Atlantic. *Deep Sea Research Part II: Topical Studies in Oceanography*, 48(13),  
170 2787-2809, 2001

171

172

173

174

175

176